Phase diagram of the half-filled one-dimensional t-V-V' model

Tapan Mishra, Juan Carrasquilla, and Marcos Rigol

Department of Physics, Georgetown University, Washington, DC 20057, USA

We study the phase diagram of spinless fermions with nearest- and next-nearest-neighbor interactions in one dimension utilizing the (finite-size) density-matrix renormalization group method. The competition between nearest- and next-nearest-neighbor interactions and nearest-neighbor hopping generates four phases in this model: two charge-density-wave insulators, a Luttinger-liquid phase, and a bond-order phase. We use finite-size scaling of the gap and various structure factors to determine the phase diagram.

I. INTRODUCTION

The study of quantum phase transitions in strongly interacting systems has become a major field of research in condensed matter physics. Quantum fluctuations, rather than thermal fluctuations, are responsible for such zero-temperature phase transitions.[1] Remarkably, quantum fluctuations play a more dominant role as the dimensionality of the system is reduced. In that sense, one and two dimensions are in general an ideal playground where the interplay between strong interactions and quantum fluctuations leads to the emergence of exotic phases and phenomena. For example, in one dimension, it is known that quantum fluctuations melt any order that would otherwise break a continuous symmetry.[2,3]

In recent years, in addition to traditional condensed matter systems that exhibit reduced dimensionalities, ultracold atomic gases in optical lattices have allowed the experimental realization of several strongly correlated systems that are of great interest.[4] The degree of control in those experiments is such that effective one-dimensional regimes are now within reach.[5] In addition, the high degree of isolation in optical lattice experiments enables the study of nonequilibrium phenomena not accessible in condensed matter settings,[7,8] and addressing questions related to the relaxation dynamics and thermalization of quantum systems.[9]

One-dimensional systems have been the focus of many recent works on the effects of integrability and phase transitions in the dynamics and thermalization of strongly interacting quantum systems.[5,6] In particular, one of us (in collaboration with L. Santos) studied the breakdown of thermalization in the t-V-V' model, and its relation to approaching integrable points and the various insulating phases present in its ground state.[10,11] Interestingly, despite the simplicity of the model, and the fact that it has been studied in several previous works,[12–17] an accurate phase diagram is not available in the literature.

In this work, we present a detailed study of the phase diagram of the t-V-V' model. For spinless fermions, in its particle-hole symmetric form, the Hamiltonian can be written as

$$H = \sum_i \left[-t\,(c_i^\dagger c_{i+1} + \text{H.c.}) + V\left(n_i - \frac{1}{2}\right)\left(n_{i+1} - \frac{1}{2}\right) \right.$$
$$\left. + V'\left(n_i - \frac{1}{2}\right)\left(n_{i+2} - \frac{1}{2}\right) \right], \qquad (1)$$

where $c_i^\dagger$ and c_i are fermionic creation and annihilation operators at site i, respectively. These operators obey the usual fermionic anticommutation relations $\{c_i, c_j^\dagger\} = \delta_{i,j}$. $n_i = c_i^\dagger c_i$ is the number operator. t is the hopping amplitude between neighboring sites, and V and V' are the nearest- and next-nearest-neighbor interactions, respectively.

We focus our analysis on the half-filled case, i.e., when the number of fermions is equal to one-half the number of lattice sites. For $V' = 0$, this Hamiltonian can be solved exactly using the Bethe ansatz.[5] As V is increased, one finds a transition from a gapless Luttinger liquid (LL) to a gapped charge-density-wave phase at $V/t = 2$. For $t = 0$, on the other hand, the ground state of model (1) is very simple (a product state) and is determined by the ratio between V and V'. For $V' < V/2$ one has a $(\ldots 10101010 \ldots)$ charge-density wave (CDW-I) and for $V' > V/2$ one has a $(\ldots 11001100 \ldots)$ charge-density wave (CDW-II). Here, 1 (0) denotes the presence (absence) of a fermion at a particular site. However, for finite values of t, a richer phase diagram emerges.

Early numerical studies of this model were based on the Lanczos method,[12] for which only small system sizes can be diagonalized. It was found that the competition between t, V, and V' leads to four different phases. Three of those phases have been already mentioned, the LL, CDW-I, and CDW-II phases. In addition to those, a bond-order (BO) phase was also found. This BO phase was somehow missed in some subsequent studies of this model.[14,15] More recently, the presence of the BO phase was discussed in a density-matrix renormalization group (DMRG) study, but the phase diagram was not computed there.[16]

It is interesting to note that despite the fact that the physics of the t-V-V' model is well understood,[5] as mentioned before, no accurate phase diagram has been reported so far. This is because large finite-size effects make it difficult to determine the precise boundaries between the phases mentioned above. In this paper, utilizing the DMRG technique, we determine the phase diagram of the t-V-V' model for a broad range of values of V/t and V'/t. In order to make accurate predictions, we use scaling properties of several quantities, which are based on the universality class of the various transitions. Our main result is the phase diagram reported in Fig. 1.

The exposition is organized as follows. In Sec. II, we discuss the model under consideration and its formulation in different physical contexts. We also introduce the observables used to describe the different ground-state phases. In Sec. III,
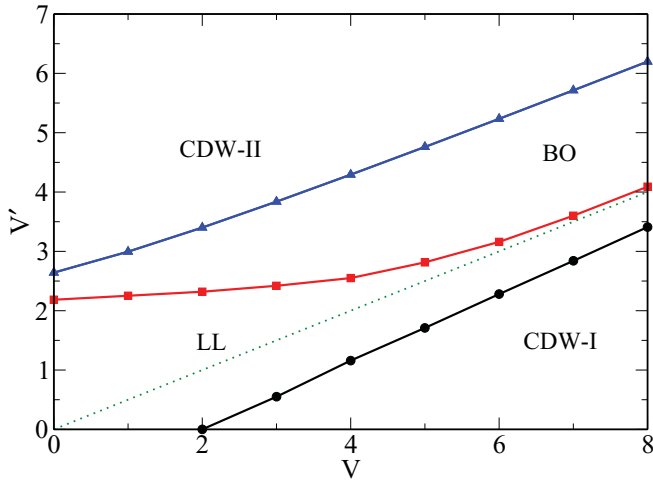
FIG. 1. (Color online) Phase diagram of the half-filled t-V-V' model. The phases are, from bottom to top, charge-density wave with a two-site unit cell, Luttinger liquid, bond-order phase, and charge-density wave with a four-site unit cell. The dashed line corresponds to $V' = V/2$, which, in the atomic limit, gives the boundary between the CDW-I and CDW-II phases. The hopping amplitude is set to $t = 1$.

we provide details on the different approaches used to detect the transitions from gapless to gapped phases. In particular, we determine the transition line from the LL to the CDW-I as well as the transition from the LL to the BO phase. In Sec. IV, the transition from the BO phase to the CDW-II is studied by performing finite-size scaling analysis of the structure factor. We also compare the obtained phase diagram with the one found in previous studies. Finally, in Sec. V, we briefly summarize our main conclusions.

II. MODEL, OBSERVABLES, AND APPROACH

The t-V-V' model for spinless fermions [Eq. (1)] can be mapped onto two other models of much interest in condensed matter and cold gases.

The first of those two models is a well-known spin chain. Using the Jordan-Wigner transformation,[18]

$$c_i^\dagger = S_i^+ \prod_{\beta=1}^{i-1} e^{i\pi(S_\beta^z + 1/2)}, \quad c_i = \prod_{\beta=1}^{i-1} e^{-i\pi(S_\beta^z + 1/2)} S_i^-,$$

$$c_i^\dagger c_i = S_i^z + \frac{1}{2}, \qquad (2)$$

where S_i^x, S_i^y, S_i^z are spin-$\frac{1}{2}$ operators at site i, the Hamiltonian (1) takes the form

$$H = \sum_i \left[-2t \left(S_i^x S_{i+1}^x + S_i^y S_{i+1}^y \right) + V S_i^z S_{i+1}^z + V' S_i^z S_{i+2}^z \right]. \qquad (3)$$

This is the spin-1/2 XXZ chain with an additional next-nearest-neighbor $S^z S^z$ interaction term. For the mapping, we have assumed that the system has open boundary conditions, as will be the case throughout this work. For periodic boundary conditions, a boundary term appears which depends on the total number of fermions (total S^z) in the chain.[19]

Furthermore, one can map the spin model above onto a model of impenetrable (hard-core) bosons, known as the lattice Tonks-Girardeau gas within the cold-gases community.[5] For this, one can use the Holstein-Primakoff transformation for spin-1/2 particles:[20]

$$S_i^+ = a_i^\dagger \sqrt{1 - a_i^\dagger a_i}, \quad S_i^- = \sqrt{1 - a_i^\dagger a_i}\, a_i,$$

$$S_i^z = a_i^\dagger a_i - \frac{1}{2}. \qquad (4)$$

Under this transformation, Eq. (3) can be written as

$$H = \sum_i \left[-t \left(a_i^\dagger a_{i+1} + \text{H.c.} \right) + V \left(n_i^b - \frac{1}{2} \right) \left(n_{i+1}^b - \frac{1}{2} \right) \right.$$

$$\left. + V' \left(n_i^b - \frac{1}{2} \right) \left(n_{i+2}^b - \frac{1}{2} \right) \right], \qquad (5)$$

where $a_i^\dagger$ (a_i) is the bosonic creation (annihilation) operator obeying the bosonic commutation relations $[a_i, a_j^\dagger] = \delta_{i,j}$ and $n_i^b = a_i^\dagger a_i$ is the bosonic number operator. One also has an additional constraint $a_i^{\dagger 2} = a_i^2 = 0$ that precludes multiple occupancies of the lattice sites.

From the derivations above, one can see that spinless fermions, spins, and hard-core bosons share the same spectrum, and diagonal (density and S^z) correlations. Hence, the phase diagram obtained in this study for spinless fermions is also relevant to the corresponding spin and bosonic models. Experimentally, hard-core bosons have been realized in one-dimensional geometries in the presence[21] and absence[22] of a lattice.

In order to compute the ground-state properties of the t-V-V' model, we use the finite-size DMRG algorithm with open boundary conditions.[23,24] This method is best suited for (quasi-)one-dimensional problems and has been extensively used to study quantum spin chains.[24] To minimize finite-size effects and obtain accurate extrapolations, we study systems with up to 700 sites (1000 in fewer cases) retaining 128 density-matrix eigenstates. The weight of the states discarded in the density matrix is less than 10^{-6} in all cases. To improve the convergence, at the end of each DMRG step, we use a finite-size sweeping procedure.[24]

To characterize the various phases of this model, we have studied several quantities. Here, we report results for the single-particle excitation gap,

$$G_L = E(L, N+1) + E(L, N-1) - 2E(L, N). \qquad (6)$$

It allows us to distinguish gapped and gapless phases. In Eq. (6), $E(L,N)$ is the ground-state energy of a system with L sites and N fermions.

To understand the transition to the CDW phases, we calculate the structure factor, which is the Fourier transform of the density-density correlation function,

$$S(k) = \frac{1}{L^2} \sum_{i,j} e^{ik(i-j)} (\langle n_i n_j \rangle - \langle n_i \rangle \langle n_j \rangle). \qquad (7)$$

Finally, the transition to the BO phase can be identified by calculating the bond-order parameter

$$O_{\text{BO}} = \frac{1}{L} \sum_i (-1)^i B_i, \qquad (8)$$

where

$$B_i = \langle c_i^\dagger c_{i+1} + c_{i+1}^\dagger c_i \rangle. \qquad (9)$$

In the remainder of the paper, we set $t = 1$.

III. GAPLESS TO GAPPED PHASE TRANSITIONS

We first focus on the transition between the gapless LL phase and the two gapped phases that surround it, which are the CDW-I and the BO phases. These two transitions can be understood using LL theory, from which one obtains that the Luttinger parameter is $K = 1/2$ at the transition points.[5] One can then use this knowledge to determine the boundaries between the LL and CDW-I/BO phases. The idea would be to compute K using the decay of correlations for finite systems, make an extrapolation to the thermodynamic limit, and then find the values of V' that for a given value of V result in $K = 1/2$. This approach was used, for example, to calculate the phase diagram of the extended Hubbard model.[25] We find that such a procedure leads to inconclusive results for the t-V-V' model. The selection of the range of distances used to fit K from correlation functions, such as the one-particle density matrix $\rho_{ij} = \langle c_i^\dagger c_j \rangle$, leads to a wide range of values of K for any given finite system. After extrapolation to the thermodynamic limit, the errors in the determination of the critical V', for each value of V, were found to be large. One could also try to use the appropriate functional form of the relevant correlation functions as obtained in low-energy effective theories, as has been done in the context of spin chains[26,27] and zigzag ladders,[28] but we have followed a different approach.

Our approach is based on the study of the closing of the single-particle excitation gap G_L [see Eq. (6)] when entering the LL phase. G_L can be accurately determined within DMRG at a relatively low computational cost (in particular, if one compares it with the cost of computing correlation functions). Of course, G_L is finite for any finite system even in phases that are gapless in the thermodynamic limit. As an example, in Fig. 2 we show LG_L as function of V' and fixed $V = 4$, for two
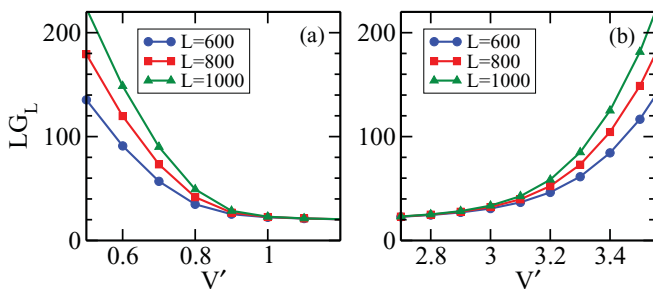

FIG. 2. (Color online) Scaling of the gap LG_L plotted as a function of V' for $V = 4.0$. The coalescence of different curves for $V' \gtrsim 1.0$ in (a) and $V' \lesssim 2.9$ (b) indicates the transition from gapped to gapless phase.
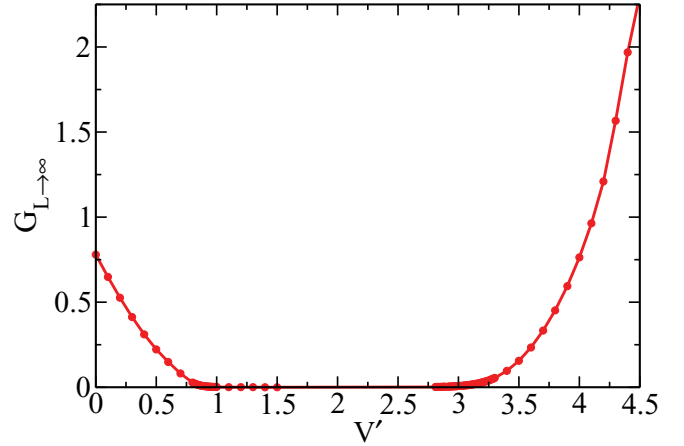

FIG. 3. (Color online) The extrapolated gap in the thermodynamic limit is plotted as a function of V' for $V = 4$. There is a transition from a gapped to a gapless phase at $V' \sim 1.0$ and then to a gapped phase again at $V' \sim 2.9$.

different intervals of V', and various system sizes. One can see there that LG_L is finite for all values of V' and all system sizes. However, in some parameter regimes LG_L does not change with increasing system size, i.e., $G_L \sim 1/L$ (vanishes in the thermodynamic limit), while in other parameter regimes, LG_L increases with increasing system size and so G_L is finite in the thermodynamic limit.

One can then extrapolate G_L to the thermodynamic limit by fitting it to a polynomial in terms of $1/L$ and obtain the value of $G_{L\to\infty}$ by varying V' for all the values of V. Results for the extrapolated gap $G_{L\to\infty}$ as a function of V' for $V = 4$ are shown in Fig. 3. This plot shows a clear transition from a gapped to a gapless phase and then to a gapped phase. The system becomes gapless at $V' \sim 1.0$ and the gap reopens at $V' \sim 2.9$. Still, within this approach, one encounters the difficulty of pinpointing the exact values of V' for the phase transition.

In order to obtain accurate values of V' for the boundaries between the gapped and gapless phases, we make use of the knowledge that the transition between the gapless and gapped phases belongs to the Berezinskii-Kosterlitz-Thouless (BKT) type.[5] At the BKT transition the gap closes as

$$G \sim \exp\left[-\frac{a}{\sqrt{|V' - V_c'|}} \right], \qquad (10)$$

where a is a constant.

The correlation length ξ, which is closely related to the gap, is finite in the gapped phase, diverges at the critical point as $\xi \sim G^{-1}$, and remains infinite in the LL phase. We utilize the following finite-size-scaling relation for the gap in the vicinity of the phase transition,

$$LG_L\left(1 + \frac{1}{2\ln L + C}\right) = F\left(\frac{\xi}{L}\right), \qquad (11)$$

where F is a scaling function and C is an unknown constant to be determined. This scaling ansatz resembles the analogous scaling relation for the resistance in the charge-unbinding transition of the two-dimensional Coulomb gas.[29] In such a transition, which is also of the BKT type, the resistance

near the critical point behaves as the gap does in the gapped to LL transition; namely, it vanishes exponentially as in Eq. (10).

At the critical point and close to it within the LL phase, one expects the values of $F(\xi/L)$ to be system-size independent because of the divergence of the correlation length; i.e., plots of $LG'_L = LG_L[1 + 1/(2\ln L + C)]$ as function of V' for different system sizes should merge in that region. Furthermore, the resulting curves of plotting LG'_L as function of ξ/L for several values of L should also be system-size independent. Equivalently, one can plot LG'_L as a function of $x_L = \ln L - \ln \xi$ to get the collapse of the curves. In our calculations, the values of a, C, and V'_c are fitted to produce the best possible collapse of the data within the gapped side of the phase transition. On that side, we take into account that the correlation length diverges as $\xi \sim \exp[a/\sqrt{|V' - V'_c|}]$. We have tested the accuracy of this procedure by determining the critical value of V for the transition between the LL and CDW-I phases when $V' = 0$. As mentioned in the introduction, the critical value of V in this case is known analytically (the Heisenberg point). We considered systems with up to 700 sites and obtained a critical value $V_c = 2.02 \pm 0.01$, which is consistent with the analytical result.

When $V' \neq 0$, this model is not exactly solvable. In Fig. 4, we show results for LG'_L vs x_L (main panels), as well as LG'_L vs V' (insets), for $V = 4$ and several values of L. The main panels make evident the collapse of all the data for the rescaled gap as a function of x_L, shown here only within the gapped phases. Two important limits can be understood by analyzing the collapse curves. As the critical point is approached ($x_L \to -\infty$), the scaling function approaches a constant value, which in turn implies the vanishing of the gap. In the limit of large x_L, one can see that the scaling function increases rapidly, which is necessary for the gap to be finite in the gapped phases. We then confirm two aspects of the BKT transition, the exponentially divergent correlation length and the logarithmic corrections to the gap. The insets in Fig. 4 clearly show that, when coming

from the gapped phases, the LG'_L curves merge at a point [$V'_c = 1.16$ for the CDW-I to LL phase, Fig. 4(a), and $V'_c = 2.55$ for the BO to LL phase, Fig. 4(b)] and remain close to each other for some finite region within the gapless phase. Moreover, as the size of the system increases, the interval over which the curves are seen to collapse within the LL phase increases. As said before, because of the divergence of the correlation length in the LL phase, the curves should be system-size independent in the vicinity of the transition point, where the scaling relation (11) holds.

A. CDW-I to LL transition

As mentioned in the introduction, only two phases are present in the system for $V' = 0$. Those are a LL phase for $0 < V < 2$ and a CDW-I phase for $V > 2$. By adding a small V', the transition between LL to the CDW-I is shifted to larger values of V, thus enhancing the stability of the LL phase. This is because the interplay between CDW configurations of the type $(\ldots 101010 \ldots)$, favored by increasing values of V, competes with those of the type $(\ldots 11001100 \ldots)$, favored by increasing values of V', thus making the system gain kinetic energy because of the net reduced charge ordering effects. Nevertheless, for large enough values of V, the CDW-I phase is prevalent. In order to see that this is the case, we have calculated the density-density structure factor $S(k)$ as defined by Eq. (7). Because of the charge order, the CDW-I phase is characterized by a finite value of $S(\pi)$ in the thermodynamic limit. In Fig. 5, we show $S(\pi)$ as function of $1/L$ for different values of V', and for $V = 4$. It is apparent in that figure that, for $V' \lesssim 1.0$, $S(\pi)$ is finite in the thermodynamic limit. For $V' \gtrsim 1.2$, on the other hand, $S(\pi)$ becomes very small as the system size increases, which suggests that it will be zero in the thermodynamic limit. This is consistent with the results from the scaling of the gap that, for $V = 4$, predicted the critical value of V' for the transition between the LL and the CDW-I phase to be $V' = 1.16$. Despite the fact that with the finite-size scaling of the structure factor $S(\pi)$ it is difficult to locate the
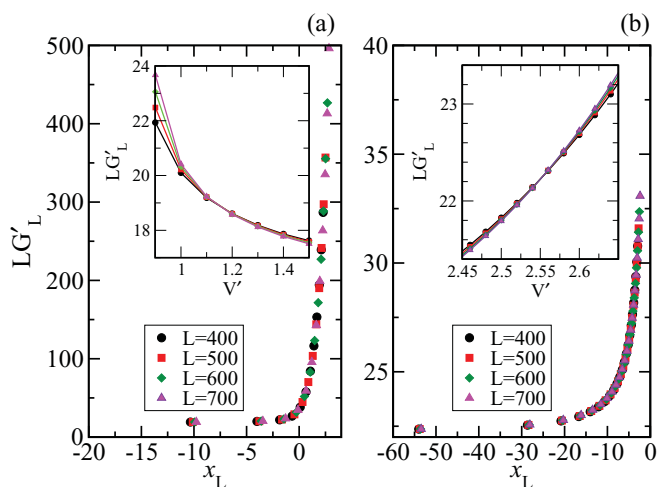
FIG. 4. (Color online) The scaled gap LG'_L as function of the $x_L = \ln L - a/\sqrt{|V' - V'_c|}$. The insets show the scaled gap as function of V'. (a) Transition from the CDW-I to the LL phase. (b) Transition from the LL to the BO phase. Both transitions are presented for a fixed value of $V = 4$.
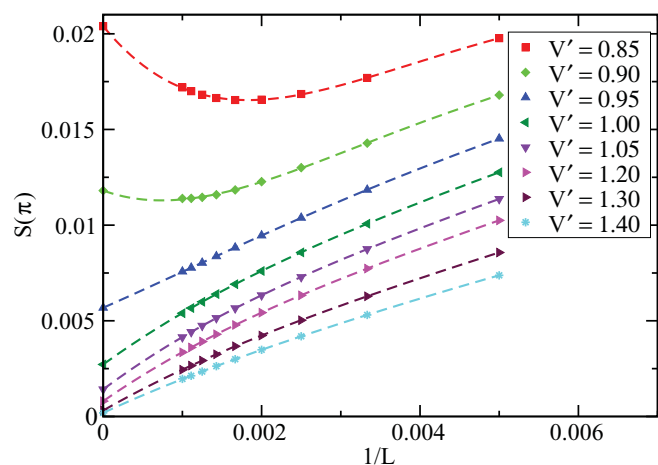
FIG. 5. (Color online) Density-density structure factor $S(\pi)$ as a function of $1/L$ for different values of V', for $V = 4$. $S(\pi)$ is predicted to be finite in the thermodynamic limit for $V' \lesssim 1.2$, making evident the existence of a CDW-I phase in that region of parameter space.
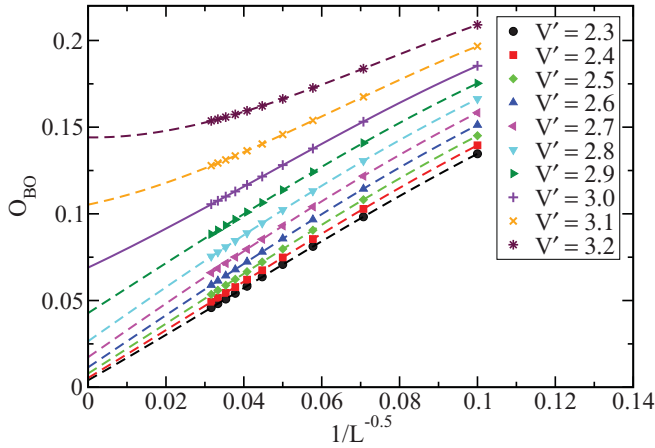
FIG. 6. (Color online) Finite-size scaling of O_{BO} for different values of V', for $V = 4$, across the LL to BO phase.

exact transition point, this calculation provides evidence of the nature of the CDW-I phase and the way the charge order develops as one crosses the critical region.

B. LL to BO transition

At the other boundary of the LL phase, when $V' > V/2$, there is an instability toward the formation of a gapped BO phase.[12,17] In the limit of vanishing V, the bond-order phase arises because of the competition between the kinetic energy term and the next-nearest-neighbor interaction that induces a CDW-II order. A finite value of V competes with the bond ordering induced by V', thus enhancing the stability of the LL phase and increasing the critical value of V'. As mentioned previously, the BO phase is characterized by a finite value of O_{BO} [see Eq. (8)] in the thermodynamic limit. Although this phase exhibits bond oscillations as unveiled by the O_{BO} parameter, the system exhibits no charge order. Therefore, two quantities can be used to characterize the BO phase, the gap and O_{BO}, which are both finite in that phase. In a finite-size
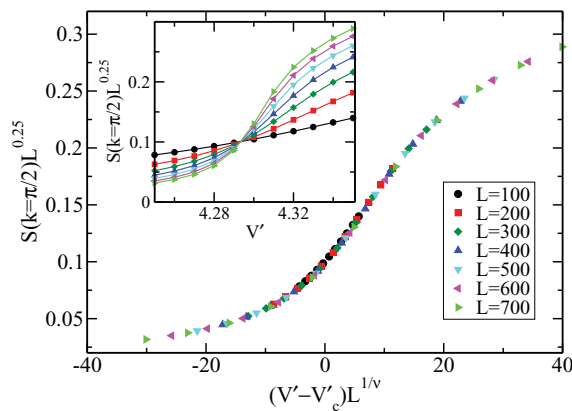

FIG. 7. (Color online) Scaled $S(\pi/2)$ vs the scaled control parameter for $V = 4$. The collapse of all the data points onto a single curve confirms the critical point at $V'_c = 4.293$. Inset: Crossing of the scaled $S(\pi/2)$ for $V = 4$ and different system sizes. All the curves intersect at $V'_c = 4.293$ indicating the transition point.
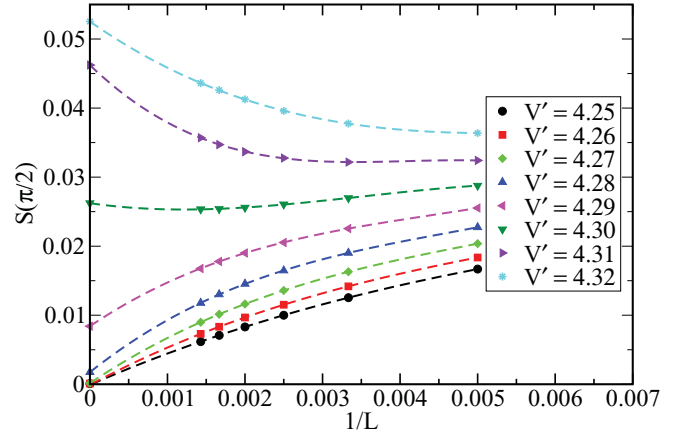

FIG. 8. (Color online) Scaling of $S(\pi/2)$ vs $1/L$ for $V = 4$ and different values of V' between $V' = 4.25$ and $V' = 4.32$ in steps of 0.01. One can see that $S(\pi/2)$ extrapolates to zero below the critical value $V'_c = 4.293$.

system, however, BO oscillations are present in the LL phase, but vanish as the system size in increased.

Following the arguments in Ref. 30 and 31, the strength of such oscillations is assumed to decay as L^{-K}. This scaling relation holds inside the LL region and in particular at the transition point between the LL and the BO phase, where the Luttinger-liquid parameter takes the value $K = 1/2$. Because of that, we extrapolate the BO parameter using $L^{-1/2}$ rather than L^{-1}. In Fig. 6, we plot O_{BO} as a function of $L^{-1/2}$ for different values of V' at $V = 4$. One can see there that O_{BO} extrapolates to a nonzero value in the thermodynamic limit for $V' \gtrsim 2.6$. Despite the large size effects that are present at the BKT transition, for values of $V' \lesssim 2.5$, O_{BO} extrapolates to very small values. These results are compatible with the critical value $V'_c = 2.55$ obtained from the finite-size-scaling analysis of the opening of the charge gap. Note that in Fig. 6, as the values of V' decrease and approach the critical value V_c, the curves become closer to straight lines. This supports our assumption that, at the transition point, the BO oscillations decay as $L^{-1/2}$.

IV. GAPPED TO GAPPED PHASE TRANSITION

A. BO to CDW-II transition

Ultimately, when V' is very large, the system always forms a CDW-II insulator as the energy of the configuration (. . .110011 . . .) becomes energetically more favorable. Hence, within the gapped region with $V' > V/2$, there is an additional phase transition between the BO and CDW-II phases. The latter phase is characterized by a finite value of $S(\pi/2)$ in the thermodynamic limit.

Taking $S(\pi/2)$ as the order parameter for the CDW-II phase, we obtain the critical point accurately by means of scaling theory. We start with the ansatz

$$S(\pi/2)L^{2\beta/\nu} = F((V' - V'_c)L^{1/\nu}), \qquad (12)$$

where β is the critical exponent corresponding to the universality class of the phase transition and ν is the correlation
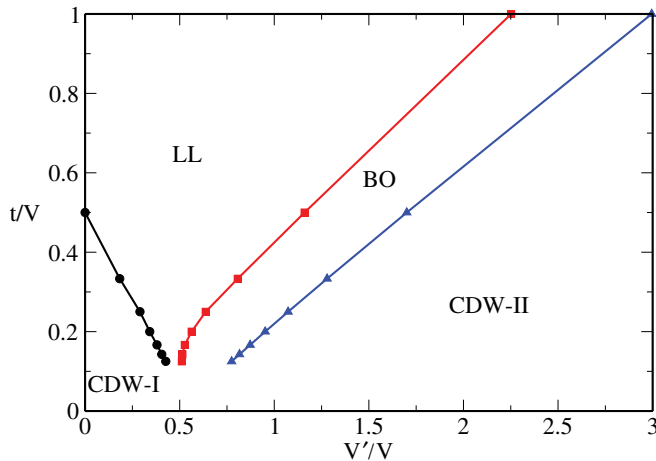
FIG. 9. (Color online) The same phase diagram as in Fig. 1 but now in the t/V vs V'/V plane.

exponent. F is a scaling function and V_c' is now the critical point for transition between the BO to CDW-II phases.

Comparing results for different system sizes as V' is changed, we found that the curves for different system sizes intersect at a unique critical point if $\beta = 0.125$ and $\nu = 1$ (these are the exponents of the 2D Ising universality class). Results for a value of $V = 4$ are shown in Fig. 7, for which $V_c' \simeq 4.293$. The scaled $S(\pi/2)$ as a function of scaled control parameter V' is plotted in Fig. 7. The collapse of the data confirms the accuracy of V_c' as determined from the crossing in the inset of Fig. 7. Notice that, as V' is increased, the transition between the BO to CDW-II occurs while the charge gap continues to grow monotonically; i.e., it does not vanish at the transition point. See the behavior of the charge gap in Fig. 3 for values around the critical $V_c' \simeq 4.293$.

In order to have an independent check that the previous approach leads to the correct results, we have also extrapolated the value of $S(\pi/2)$ to thermodynamic limit. The results from this procedure, once again for $V = 4$, are presented in Fig. 8. There, we plot $S(\pi/2)$ vs $1/L$ for different values of V'. The values of the extrapolated $S(\pi/2)$ clearly converge to zero for $V < V_c'$.

A complete analysis like the one presented so far, but for different values of V, allowed us to determine the phase diagram presented in Fig. 1.

Finally, to allow for a direct comparison with early calculations for this model, reported in Refs.[12,17], we present in Fig. 9 the phase diagram in the plane t/V-V'/V. This phase diagram is in qualitative agreement with the one reported in Refs. 12 and 17. However, quantitative differences on the precise location of the phase boundaries are apparent. Although we did not study the region of the phase diagram where $t/V \to 0$, the trend of our transition lines suggests that they will cross for small but finite values of t/V, implying a tricritical point.[12,17]

V. CONCLUSION

We have presented a comprehensive study of the phase diagram of the t-V-V' model in one dimension. Using the scaling of the gap in the BKT transition between the LL phase and the CDW-I/BO phases, we have obtained accurate results for the boundaries between the gapless and gapped phases of this model, which are confirmed by the extrapolation of various order parameters. The phase transition between the BO phase and the CDW-II phase (both of which are gapped) was also studied using scaling theory for the density-density structure factor. This latter phase transition was found to be much less sensitive to finite-size effects and the exponents computed were found to be consistent with those of the two-dimensional Ising universality class.

[1] S. Sachdev, *Quantum Phase Transitions* (Cambridge University Press, Cambridge, 2002).

[2] P. C. Hohenberg, Phys. Rev. **158**, 383 (1967).

[3] N. D. Mermin and H. Wagner, Phys. Rev. Lett. **17**, 1133 (1966).

[4] I. Bloch, J. Dalibard, and W. Zwerger, Rev. Mod. Phys. **80**, 885 (2008).

[5] M. A. Cazalilla, R. Citro, T. Giamarchi, E. Orignac, and M. Rigol, e-print arXiv:1101.5337.

[6] A. Polkovnikov, K. Sengupta, A. Silva, and M. Vengalattore, Rev. Mod. Phys. **83**, 863 (2011).

[7] T. Kinoshita, T. Wenger, and D. S. Weiss, Nature (London) **440**, 900 (2006).

[8] S. Trotzky, Y.-A. Chen, A. Flesch, I. P. McCulloch, U. Schollwöck, J. Eisert, and I. Bloch, e-print arXiv:1101.2659.

[9] M. Rigol, V. Dunjko, and M. Olshanii, Nature (London) **452**, 854 (2008).

[10] M. Rigol and L. F. Santos, Phys. Rev. A **82**, 011604(R) (2010).

[11] L. F. Santos and M. Rigol, Phys. Rev. E **82**, 031130 (2010).

[12] K. Hallberg, E. Gagliano, and C. Balseiro, Phys. Rev. B **41**, 9474 (1990).

[13] K. Nomura and K. Okamoto, J. Phys. A: Math. Theor. **27**, 5773 (1994).

[14] A. K. Zhuravlev, M. I. Katsnelson, and A. V. Trefilov, Phys. Rev. B **56**, 12939 (1997).

[15] D. Poilblanc, S. Yunoki, S. Maekawa, and E. Dagotto, Phys. Rev. B **56**, R1645 (1997).

[16] P. Schmitteckert and R. Werner, Phys. Rev. B **69**, 195115 (2004).

[17] V. J. Emery and C. Noguera, Phys. Rev. Lett. **60**, 631 (1988).

[18] P. Jordan and E. Wigner, Z. Phys. **47**, 631 (1928).

[19] E. Lieb, T. Shultz, and D. Mattis, Ann. Phys. (NY) **16**, 406 (1961).

[20] T. Holstein and H. Primakoff, Phys. Rev. **58**, 1098 (1940).

[21] B. Paredes, A. Widera, V. Murg, O. Mandel, S. Fölling, I. Cirac, G. V. Shlyapnikov, T. W. Hänsch, and I. Bloch, Nature (London) **429**, 277 (2004).

[22] T. Kinoshita, T. Wenger, and D. S. Weiss, Science **305**, 1125 (2004).

[23] S. R. White, Phys. Rev. Lett. **69**, 2863 (1992).

[24] U. Schollwöck, Rev. Mod. Phys. **77**, 259 (2005).

[25] T. D. Kühner, S. R. White, and H. Monien, Phys. Rev. B **61**, 12474 (2000).

[26] T. Vekua, A. Honecker, H.-J. Mikeska, and F. Heidrich-Meisner, Phys. Rev. B **76**, 174420 (2007).

[27] T. Hikihara and A. Furusaki, Phys. Rev. B **69**, 064427 (2004).

[28] T. Hikihara, T. Momoi, A. Furusaki, and H. Kawamura, Phys. Rev. B **81**, 224433 (2010).

[29] M. Wallin and H. Weber, Phys. Rev. B **51**, 6163 (1995).

[30] S. Ejima and S. Nishimoto, Phys. Rev. Lett. **99**, 216403 (2007).

[31] S. R. White, I. Affleck, and D. J. Scalapino, Phys. Rev. B **65**, 165122 (2002).